A CAR FOLLOWING MODEL WITH AN ATTENTION-BASED COGNITIVE FRAMEWORK: THEORY, APPLICATION, AND STATISTICAL ANALYSIS

A THESIS SUBMITTED TO

THE GRADUATE SCHOOL OF ENGINEERING AND SCIENCE

OF BILKENT UNIVERSITY

IN PARTIAL FULFILLMENT OF THE REQUIREMENTS FOR

THE DEGREE OF

MASTER OF SCIENCE

IN

MECHANICAL ENGINEERING

By

Şeymanur Al Habboush

August 2024

A CAR FOLLOWING MODEL WITH AN ATTENTION-BASED COGNITIVE FRAMEWORK: THEORY, APPLICATION, AND STATISTICAL ANALYSIS

By Şeymanur Al Habboush

August 2024

We certify that we have read this thesis and that in our opinion it is fully adequate, in scope and in quality, as a thesis for the degree of Master of Science.

Yıldıray Yıldız(Advisor)

İsmail Uyanık

Gökberk Kabacaoğlu

Approved for the Graduate School of Engineering and Science:

Orhan Arıkan
Director of the Graduate School

ABSTRACT

A CAR FOLLOWING MODEL WITH AN ATTENTION-BASED COGNITIVE FRAMEWORK: THEORY, APPLICATION, AND STATISTICAL ANALYSIS

Şeymanur Al Habboush
M.S. in Mechanical Engineering
Advisor: Yıldıray Yıldız
August 2024

Traffic simulators are essential for testing autonomous driving algorithms, and they require driver models that accurately emulate human behavior to reflect real traffic conditions. This thesis focuses on developing human driver models to be used in these simulators. The limitations of fixed driver models, which do not adapt to new information, are addressed by introducing an attention-based learning mechanism inspired by human memory. This mechanism is integrated into a multi-type car-following model developed in this study. Unlike existing models, this approach allows the ego driver's decisions to be influenced by both the vehicle in front and the driver behind them.

The predictive capabilities of the proposed model is demonstrated using human driving data and a comprehensive statistical analysis of the model parameter distributions is provided. This analysis shows how the model captures general behavioral tendencies across different data sets, enhancing the understanding of interactions between human drivers and providing more realistic simulations for testing purposes. Finally, a step by step guide for using the model in the development of high-fidelity traffic models is presented.

Keywords: Human memory, learning, adaptation, car following model, adaptive control applications .

ÖZET

DİKKATE DAYALI BİLİŞSEL YAPIYA SAHİP BİR ARAÇ TAKİP MODELİ: TEORİ, UYGULAMA VE İSTATİSTİKSEL ANALİZ

Şeymanur Al Habboush
Makine Mühendisliği, Yüksek Lisans
Tez Danışmanı: Yıldıray Yıldız
Ağustos 2024

Trafik simülatörleri, otonom sürüş algoritmalarını test etmek için esastır ve gerçek trafik koşullarını yansıtmak için insan davranışını doğru bir şekilde taklit eden sürücü modelleri gerektirir. Bu tez, bu simülatörlerde kullanılacak insan sürücü modellerinin geliştirilmesine odaklanmaktadır. Yeni bilgilere uyum sağlamayan sabit sürücü modellerinin sınırlamaları, insan hafızasından esinlenen dikkat tabanlı bir öğrenme mekanizmasının tanıtılmasıyla ele alınmaktadır. Bu mekanizma, bu çalışmada geliştirilen çok tipli bir araç takip modeline entegre edilmiştir. Mevcut modellerin aksine, bu yaklaşım ego sürücüsünün kararlarının hem önündeki araçtan hem de arkasındaki sürücüden etkilenmesine olanak tanır.

Önerilen modelin öngörü yetenekleri, insan sürüş verileri kullanılarak gösterilmiş ve model parametre dağılımlarının kapsamlı bir istatistiksel analizi sağlanmıştır. Bu analiz, modelin farklı veri kümelerindeki genel davranış eğilimlerini nasıl yakaladığını, insan sürücüler arasındaki etkileşimlerin anlaşılmasını nasıl geliştirdiğini ve test amaçları için daha gerçekçi simülasyonlar sağladığını göstermektedir. Son olarak, modelin yüksek doğruluklu trafik modellerinin geliştirilmesinde kullanılmasına yönelik adım adım bir kılavuz da bu tezin sonunda yer almaktadır.

Anahtar sözcükler: İnsan hafızası, öğrenme, adaptasyon, araç takip modeli, adaptif kontrol uygulamaları.

Acknowledgement

As I proudly complete the first step of the journey of academia, I would like to thank the invaluable people who have supported and guided me along the way. To begin with, I would like to express my deepest gratitude to my advisor, Assoc. Prof. Yıldıray Yıldız, for his invaluable guidance throughout my academic journey. His original ideas illuminated the path forward whenever my research hit an impasse, and his unwavering support was instrumental to my success. I also thank Asst. Prof. Gökberk Kabacaoğlu for sparking my interest in diverse subjects and broadening my academic perspective, and Assoc. Prof. İsmail Uyanık for his insightful comments during my thesis defense.

I would like to express my gratitude to my friends in the graduate office for making this journey more manageable. Additionally, my special thanks go to Zeynep and Özge for their continuous support throughout my bachelor's and master's studies. Your friendship made everyday at school a joy.

I wholeheartedly thank my parents, Serap and Kadir, who have been my greatest supporters. Their unwavering presence and emotional support have been the foundation of my strength throughout this journey. To my brother, Emre, thank you for bringing joy into my life and completing our family. Without you, my life would be far less colorful.

Finally, I want to express my heartfelt gratitude to my husband, Abdullah, the unsung hero behind my success. Your unwavering love and support have been my anchor through this journey. With you by my side, I feel motivated to take on new challenges. I am truly grateful for every moment we share and for the incredible happiness you bring into my life. I am so thankful that our paths crossed, and I look forward to all the adventures ahead of us.

Contents

List of Figures

List of Tables

List of Symbols

n	Number of vehicles of interest
m	Vehicle index, $m \in \{1, \ldots, n\}$
j	Index of observed drivers, for car following models, it can be f for the vehicle in front or b for the vehicle at the back
l	Number of driving types
i	Driving type, $i \in \{1, \ldots, l\}$
i^*	Best driving type against driving type i
α	Preferred front distance to back distance ratio
α_m	Preferred front distance to back distance ratio for m^{th} vehicle
$\alpha^{(i)}$	Preferred front distance to back distance ratio associated with driving type i
I_i	Ratio interval associated with driving type i
$v_i(\cdot)$	Value function associated with driving type i
r_{j_t}	Front distance to back distance ratio of observed driver j at time instant t
M_{ji}	Memory sub-unit dedicated to driving type i in memory unit allocated to observed driver j
T_{ji}	Type score for observed driver j to be of type i

θ_f Attention parameter representing ego driver's attention rate to the vehicle in front

θ_{ego} Self-attention parameter representing ego driver's tendency to stay in the initial driving style

θ_b Attention parameter representing ego driver's attention rate to the vehicle at back

γ Learning rate of the ego driver

Chapter 1

Introduction

In the epoch that autonomous cars started to be part of our lives, the research conducted for their improvement gained more importance. One of the most important aspects to consider in the development of autonomous driving algorithms is the fact that until the transition to fully autonomous traffic flow is complete, autonomous vehicles will share the roads with human drivers. For this reason, the safety of mixed traffic, consisting of both autonomous and human drivers, must be ensured.

Demonstrating that autonomous vehicles are as safe as human-driven ones requires operating them at least hundreds of millions of miles without any major incidents [1]. Conducting high-fidelity simulation tests has the potential to significantly accelerate this process. Furthermore, simulators provide the opportunity to test various scenarios –including edge cases that can rarely be experienced in real traffic– at a significantly higher speed compared to real traffic tests. Since driver models are the backbones of these simulators, modeling human driving behavior realistically is of key importance in autonomous vehicle research [2].

In this thesis, inspired by *the modal model* of human memory [3, 4] –a well-established theoretical model in cognitive psychology–, a human-like learning

mechanism of drivers is developed, and incorporated into a multi-type attention-based car-following model. This integrated approach is designed to capture diverse driver behaviors. The memory architecture is used to store the observed data of the interacted vehicles, which is then used to continuously estimate their driving types. Then, the best driving strategy is determined using attention parameters. Since abrupt transitions between driving strategies are unrealistic, we employ an adaptive mechanism that progressively adjusts the existing strategy towards the chosen one, reflecting the learning period of humans. While presented in the context of car following models, the proposed architecture can be generalized to other multi-type driver models. In addition to human driver modeling, the proposed framework can be used in autonomous vehicle control algorithms for predicting the behavior of the surrounding vehicles.

1.1 Literature Review on Car Following Models

Classical car following models such as the GIPPS driver model [5] and intelligent driver model (IDM) [6] have significantly influenced the research in the field of traffic flow and driver modeling for a long time. Later on, recognizing the behavioral differences of human drivers during the acceleration and deceleration phases, Yeo and Skabardonis introduced the asymmetric traffic theory [7]. This theory attracted researchers working in this field, leading to the development of several models such as [8] and [9] that incorporate the asymmetry.

Unlike the studies above, certain other research has concentrated on utilizing human-generated data to capture human drivers' distinctive characteristics or classify their car-following behaviors. In [10], the Wiedemann car-following model [11] is calibrated using human driving data, and a human-like decision-making and control algorithm is developed. In [12], driver braking and acceleration behaviors are clustered to obtain driving modes such as "middle-range approaching", "collision avoidance", and "middle, short, and long-range following". Similarly, in [13], drivers are classified as radical, conservative, and calm.

Although the car following models mentioned above have been developed and used successfully in scenarios involving only human drivers, other studies developed models for traffic scenarios that include multiple autonomous vehicles or mixed traffic where human drivers and autonomous vehicles coexist. For example, various car following models are developed for connected automated vehicles [14, 15, 16, 17]. On the other hand, models such as [15, 18, 19, 20, 21, 22] are proposed for the mixed traffic environment containing human drivers together with automated vehicles.

Most of the models mentioned above are fixed, meaning they do not account for how human drivers adjust their driving style in response to interactions with surrounding vehicles. To include this effect in the model and enable the driver model to update itself online, machine learning algorithms are employed in several studies [23, 24, 25], leading to the idea of continual learning [26, 27]. In addition, algorithms such as Recurrent Neural Networks (RNN) and Long Short-term Memory (LSTM) are used in driver models benefiting from their ability to store and use historical data [28, 29]. These approaches allow driver models to use not only their current states but also their previous states in determining their future actions. However, these approaches often fail to capture the diversity of driver behaviors, as they typically rely on a limited number of model parameters for all drivers within a traffic setting. Moreover, they do not fully integrate the cognitive process of learning as it occurs in real-world driving scenarios. This gap in the literature motivates the present work, which seeks to develop a more comprehensive model that not only utilizes historical data but also simulates cognitive processes such as learning and attention. The following section outlines the specific contributions of this thesis, emphasizing the advancements and novel insights it offers compared to existing methodologies.

1.2 Contributions

In line with improving the cognitive abilities of driver models, the developed car following model with attention-based learning mechanism distinguishes itself from

existing models including those based on RNN and LSTM, in several important ways:

1. While other models use memory structures to leverage previously measured data, our model goes further by making inferences about observed drivers and incorporating these inferences into the learning phase. This capability allows our model to learn dynamically, similar to human drivers, and handle complex situations involving interactions with multiple vehicles efficiently. This is achieved by re-configuring the *modal model* of human memory, which is a well-established theoretical explanation of the data storage and processing system of human memory [3, 4], for driver modeling. Inspired by the modal model, our work mimics the structure of human memory and incorporates it into an attention-based learning framework to model the learning process of human drivers.

2. Unlike data-driven approaches that rely on complex training processes, our model incorporates a human-like memory architecture into a physics-based car following model. Physics-based models are computationally cheaper and do not require extensive training, making them more practical for real-time applications.

3. Existing models typically neglect the influence of the vehicle behind the ego vehicle, except a few such as [30, 31]. Our model, however, utilizes data from both the vehicle in front and the vehicle behind. This inclusion is crucial for accurately representing the effects of the vehicle behind, which can significantly impact the ego vehicle's behavior. In [30, 31], the impact of the vehicle in front is assumed to be larger than the impact of the vehicle at the back. In the proposed model, this assumption is eliminated. Instead, with the help of the attention mechanism, the influences of surrounding vehicles are dynamically and naturally weighed. This ensures a more accurate representation of their impact.

4. One of the most significant differences is our model's ability to represent a wide range of driver behaviors. While other models often use a single model or a few models to represent all drivers, our approach provides a

distribution of parameters that allows for the simulation of diverse driving styles. This diversity is essential for developing realistic traffic simulators where each driver behaves differently.

These contributions pave the way for designing driver models that accurately reflect human capabilities, such as interpreting information, learning, adapting to changing conditions, and exhibiting diverse behaviors.

1.3 Organization of the Thesis

This thesis is divided into chapters, each progressively building on the previous content to provide a comprehensive understanding of the developed model. It begins with the construction of a multi-type car following model, advances through the integration of a cognitive learning mechanism into it, and concludes with simulations and applications. The following is an outline of the thesis structure, detailing the key components of each chapter.

The developed multi-type car following model is introduced in Chapter 2. This chapter explains the necessity of multi-type models and presents a method for reducing model complexity. The multi-type model serves as the foundation for the car following model with learning abilities developed throughout this thesis.

Modeling human learning requires an examination of the underlying mechanisms. In Chapter 3, we detail the architecture of the memory unit inspired by the modal model. This architecture is then integrated into an attention mechanism. Along with adaptive control methodologies, these components form the overall driver model with learning abilities. The chapter concludes with proof of stability for the developed model.

Chapter 4 describes the simulation setup, parameter identification process, and analysis of parameter distributions. Comparative results between the developed

model and a conventional car following model (IDM) are provided. The performance improvements resulting from integrating the attention-based learning mechanism into the multi-type model developed in Chapter 2 are also demonstrated.

In Chapter 5, we classify parameters into groups that facilitate the construction of a traffic simulation. Two classification methods —k-means clustering and Gaussian Mixture Model— are employed, each offering distinct advantages for simulator design. The chapter concludes with a guide to the simulator design process, assisting researchers in implementing the developed car following model.

Finally, Chapter 6 summarizes the thesis, highlighting the key contributions and suggesting directions for future research.

Chapter 2

Multi-Type Car Following Model

2.1 Construction of the Model

Consider a group of n vehicles in a single lane, which we call the *vehicles of interest* and index each by $m \in \{1, \ldots, n\}$ in the sequel. It is assumed that the vehicles of interest are led by an additional vehicle at the very front, with an index number 0, and followed by another additional vehicle at the very back, with an index number $n+1$. These vehicles at the very front and at the very back are assumed to have known motion profiles, which can be obtained, for example, from traffic data.

Let the position, velocity, and acceleration of the m^{th} vehicle be denoted by $x_m(t)$, $\dot{x}_m(t)$, and $\ddot{x}_m(t)$, respectively. Referring to the vehicles in front of and at the back of the m^{th} vehicle by indices $m-1$ and $m+1$ respectively, relative distances and velocities can be expressed as

$$\Delta x_m(t) = x_{m-1}(t) - x_m(t) \tag{2.1a}$$

$$\Delta \dot{x}_m(t) = \dot{x}_{m-1}(t) - \dot{x}_m(t). \tag{2.1b}$$

Definition 1: The preferred ratio of front distance to back distance for the driver of the m^{th} vehicle is a design parameter and denoted by $\alpha_m = (\frac{\Delta x_m(t)}{\Delta x_{m+1}(t)})_{pref}$.

Using (2.1a), (2.1b), and the parameter α_m defined in Definition 1, we assign the acceleration of the m^{th} vehicle as

$$\ddot{x}_m(t) = (\Delta\dot{x}_m(t) - \alpha_m\Delta\dot{x}_{m+1}(t)) + (\Delta x_m(t) - \alpha_m\Delta x_{m+1}(t)). \tag{2.2}$$

The states of m^{th} vehicle are defined as

$$X_m(t) = \begin{bmatrix} \Delta x_m(t) \\ \dot{x}_m(t) \end{bmatrix}. \tag{2.3}$$

Then, using (2.1)-(2.3), we obtain that

$$\dot{X}_m(t) = AX_m(t) + bu_{1m}(t) - \alpha_m G(X_m(t) + u_{2m}(t)), \tag{2.4}$$

where A, G and b are defined as

$$A = \begin{bmatrix} 0 & -1 \\ 1 & -1 \end{bmatrix}, \quad G = \begin{bmatrix} 0 & 0 \\ -1 & 1 \end{bmatrix}, \quad b = \begin{bmatrix} 1 \\ 1 \end{bmatrix}, \tag{2.5}$$

and

$$\begin{aligned} u_{1m}(t) &= \dot{x}_{m-1}(t), \\ u_{2m}(t) &= \begin{bmatrix} \dot{x}_{m+1}(t) \\ x_{m-1}(t) - x_{m+1}(t) \end{bmatrix} \end{aligned} \tag{2.6}$$

are the inputs for the m^{th} vehicle.

By using (2.3) and (2.4), the dynamics of the system consisting of $n+2$ vehicles (n-many vehicles of interest, one leading and one trailing vehicles with indices 0 and $n+1$, respectively) can be written as

$$\dot{\bar{X}}(t) = \bar{A}\bar{X}(t) + B\bar{u}(t), \tag{2.7}$$

where

$$\bar{X}(t) = \begin{bmatrix} \Delta x_1(t) & \dots & \Delta x_n(t) & \dot{x}_1(t) & \dots & \dot{x}_n(t) \end{bmatrix}^T \tag{2.8}$$

is the state vector, $\bar{A} \in \mathbb{R}^{2n\times 2n}$ is a matrix of the form

$$\bar{A} = \begin{bmatrix} 0_{n\times n} & M_3 \\ M_1 & M_2 \end{bmatrix} \tag{2.9}$$

with M_1, M_2 and $M_3 \in \mathbb{R}^{n\times n}$, and $B \in \mathbb{R}^{2n\times 3}$. These matrices are defined as

$$M_1 = \begin{bmatrix} 1 & -\alpha_1 & 0 & 0 & \dots & 0 & 0 & 0 \\ 0 & 1 & -\alpha_2 & 0 & \dots & 0 & 0 & 0 \\ & \vdots & & & \ddots & & \vdots & \\ 0 & 0 & 0 & 0 & \dots & 1 & -\alpha_{n-2} & 0 \\ 0 & 0 & 0 & 0 & \dots & 0 & 1 & -\alpha_{n-1} \\ \alpha_n & \alpha_n & \alpha_n & \alpha_n & \dots & \alpha_n & \alpha_n & \beta_n \end{bmatrix}, \tag{2.10}$$

$$M_2 = \begin{bmatrix} -\beta_1 & \alpha_1 & 0 & 0 & \dots & 0 & 0 & 0 \\ 1 & -\beta_2 & \alpha_2 & 0 & \dots & 0 & 0 & 0 \\ 0 & 1 & -\beta_3 & \alpha_3 & \dots & 0 & 0 & 0 \\ & \vdots & & & \ddots & & \vdots & \\ 0 & 0 & 0 & 0 & \dots & 1 & -\beta_{n-1} & \alpha_{n-1} \\ 0 & 0 & 0 & 0 & \dots & 0 & 1 & -\beta_n \end{bmatrix}, \tag{2.11}$$

$$M_3 = \begin{bmatrix} -1 & 0 & 0 & \dots & 0 & 0 & 0 \\ 1 & -1 & 0 & \dots & 0 & 0 & 0 \\ 0 & 1 & -1 & \dots & 0 & 0 & 0 \\ & \vdots & & \ddots & & \vdots & \\ 0 & 0 & 0 & \dots & 1 & -1 & 0 \\ 0 & 0 & 0 & \dots & 0 & 1 & -1 \end{bmatrix}, \tag{2.12}$$

where $\beta_j = 1 + \alpha_j$ for all $j = 1, \dots, n$ and

$$B = \begin{bmatrix} 1 & 0 & 0 \\ 0 & 0 & 0 \\ & \vdots & \\ 0 & 0 & 0 \\ 1 & 0 & 0 \\ 0 & 0 & 0 \\ & \vdots & \\ 0 & 0 & 0 \\ 0 & \alpha_n & -\alpha_n \end{bmatrix} \tag{2.13}$$

with 1's at the 1^{st} and the $n+1^{th}$ rows. Furthermore, the input vector $\bar{u}(t) \in \mathbb{R}^3$

in (2.7) is given as

$$\bar{u}(t) = \begin{bmatrix} \dot{x}_0(t) \\ \dot{x}_{n+1}(t) \\ x_0(t) - x_{n+1}(t) \end{bmatrix}. \tag{2.14}$$

In a traffic configuration where the vehicles at the very front and at the very back, with indices 0 and $n+1$, are moving at equal and constant velocities, $\dot{x}_0(t) = \dot{x}_{n+1}(t) = \dot{x}_0$, the input vector given in (2.14) is a constant, i.e. $\bar{u}(t) = \bar{u}$. Since $\bar{A}$ is a stable matrix (see (2.9) and the Appendix), this traffic configuration is stable and converges to an equilibrium state, which, by using (2.7), can be calculated as

$$\lim_{t\to\infty} \bar{X}(t) = -\bar{A}^{-1}B\bar{u} = \begin{bmatrix} (\prod_{m=1}^{n} \alpha_m)(x_0 - x_{n+1})/\alpha_c \\ (\prod_{m=2}^{n} \alpha_m)(x_0 - x_{n+1})/\alpha_c \\ \vdots \\ (\prod_{m=n}^{n} \alpha_m)(x_0 - x_{n+1})/\alpha_c \\ \dot{x}_0 \\ \vdots \\ \dot{x}_0 \end{bmatrix}, \tag{2.15}$$

where

$$\alpha_c = 1 + \sum_{k=1}^{n} (\prod_{m=1}^{k} \alpha_{n-m+1}). \tag{2.16}$$

It is noted that the distance between the n^{th} and $n+1^{th}$ vehicles does not appear in (2.15) and can be found as $x_n - x_{n+1} = (x_0 - x_{n+1})/\alpha_c$. Therefore, all vehicles with indices $m \in \{1, \ldots, n\}$ in this configuration adhere to their preferred front-to-back distance ratios α_m (see Definition 1) since

$$\frac{\lim_{t\to\infty} \Delta x_m(t)}{\lim_{t\to\infty} \Delta x_{m+1}(t)} = \alpha_m, \tag{2.17}$$

and have equal velocities $\lim_{t\to\infty} \dot{x}_m(t) = \dot{x}_0$.

2.2 Complexity Reduction

The analysis at the end of the previous section reveals that in an equilibrium state, the ratio of the front and back vehicle distances for each vehicle may be different since the vehicles have individual α_m parameters. This results in a *multi-type model*, allowing the representation of different driving types. In contrast to the *multi-type model*, setting the parameters α_m for all $m \in \{1, \ldots, n\}$ to the same value α results in a *single-type model*, where all the drivers prefer to keep the same front to back distance ratio, which is insufficient to represent the diversity in driving styles.

Remark 1: As using the same preferred distance ratio parameter α (see Definition 1) for all drivers is insufficient to represent the diverse driving styles, assigning a unique parameter α for each and every n-many drivers is inefficient since it introduces over-parameterization leading to unnecessary complexity. To reduce the complexity, we limit the number of different driving types by $l < n$. Therefore, l-many different $\alpha^{(i)}$ values are considered in the rest of the paper, where $\alpha^{(i)}$ denotes the preferred front to back distance ratio of a type-i driver. For instance, the preferred front to back distance ratio by a type-2 driver is denoted by $\alpha^{(2)}$. Therefore, in a setting with n-many vehicles of interest, each α_m, $m \in \{1, \ldots, n\}$, is mapped with one of the $\alpha^{(i)} \in \{\alpha^{(1)}, \ldots, \alpha^{(l)}\}$ and the model with l-many driving types is obtained.

Chapter 3

Attention-based Learning Mechanism

Driving with a fixed type (see Remark 1) may not be realistic in real traffic, especially when interactions between drivers, either human or autonomous, are considered. In this chapter, an attention-based learning mechanism is introduced, which is constructed by taking into account that the types of drivers change depending on the inferences they make about the driving types of other drivers. First, the human-like memory architecture which is used to make these inferences are described. Then, the multi-type car following model described in Chapter 2 is brought into a more specific form to facilitate the incorporation of the memory structure. Finally, all components are integrated to unveil an attention-based learning mechanism that models the transition between drivers' driving styles. The flow chart of the proposed learning model is given in Fig. 3.1.

It is noted that the following procedure is valid for all the vehicles of interest and should be applied to each of them individually. However, for the simplicity of the notations, the discussion focuses on a single driver whose learning period is modeled. In the rest of the section, this driver is called the *ego driver*, and the vehicle driven by the ego driver is called the *ego vehicle*.

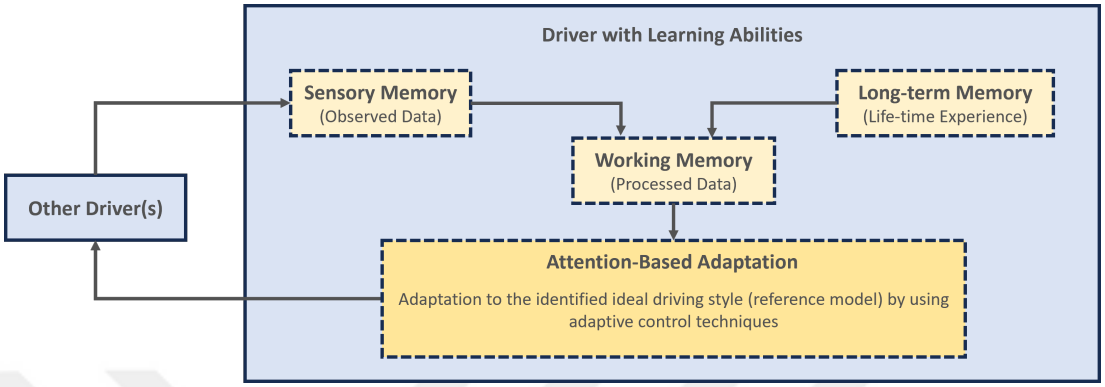

Figure 3.1: Flow chart of the proposed learning mechanism.

3.1 Human-like Memory Architecture

The *modal model*, introduced by Atkinson and Shiffrin [3], describes the structural components and processes that control the memory storage system. Since its first introduction, this model has been a foundational and influential framework in cognitive psychology research [4]. In this work, we use a memory structure that is inspired from the modal model to capture the information storage and processing characteristics of human drivers.

In this model, the repositories known as *memory stores* are responsible for holding acquired information. These memory stores are categorized into three types: *sensory memory*, *long-term memory*, and *working memory*. The type of memory where information is stored depends on its content.

The momentary storage part of the memory is called the sensory memory. Before sending it to the working memory to be processed, it keeps the information for a short time (1 second). In the memory structure we build, the information that the ego driver's sensory memory receives is the front distance to back distance ratio r_{j_t} of the observed vehicle j at time instant t. Here, the "front distance" is the distance from the observed vehicle to the vehicle in front of it. Similarly, the "back distance" is the distance from the observed vehicle to the vehicle behind it. This information is collected by the ego driver from each of the surrounding vehicle drivers separately. For the car following model described in Chapter 2,

only the information coming from the front and back vehicles is needed.

Long-term memory is the lifetime storage of important information such as facts, concepts, rules, and personal experiences. Different driving types, related to different preferred front to back distance ratios (see Remark 1), are the knowledge obtained with experience by observing other drivers. Relating observed data with one of the driving types requires an evaluation of data. It is assumed that value functions $v_i(\cdot)$ determining the probability of the observed driver to be of type-i based on observed front distance to back distance ratio exist in the long-term memory. We explain how to build these functions later in the paper. Another information that is stored in the long-term memory is the knowledge of best driving type (best response) against each driving type, definition of which is given below.

Definition 2: Consider Remark 1. The best response to driving type i is denoted by type i^* and called the *best type* against type i. The associated preferred front distance to back distance ratio for type i^* is defined as $\alpha^{(i^*)} = 1/\alpha^{(i)}$ where $\alpha^{(i)}$ is the preferred ratio parameter for type i.

Remark 2: The rationale behind Definition 2 is explained as follows. Consider an extended string of vehicles, having a pattern of alternating driving types i followed by i^*. In this arrangement, the distances between the vehicles stay stable, without diverging to infinity or vanishing to zero, which is a desired situation. This best type assignment is also supported by traffic data. Examining 500 drivers' data in the NGSIM data set [32], three driving types defined by $\alpha^{(1)} = 0.5$, $\alpha^{(2)} = 1$ and $\alpha^{(3)} = 2$ are determined with tolerances around them assigned by using geometric means $\mu_g(0.5, 1) = 0.7$ and $\mu_g(1, 2) = 1.4$. Therefore, the interval $(0.3, 0.7)$ is matched with type-1, $(0.7, 1.4)$ is matched with type-2, and $(1.4, 2.6)$ is matched with type-3 by using the symmetry around $\alpha^{(1)}$ and $\alpha^{(3)}$ values. The percentage of cases where the α values of the vehicles correspond to types 3, 2, and 1, when the vehicles in front and at the back of them have types 1, 2, and 3 (best types against them), respectively, are investigated. It turns out that this type of alignment occurs for 49.27%, 71.27% and 52.46% of available data instances, respectively. These values are significantly higher than the expected

value 33.33%, if the driving type distributions were uniformly random.

Working memory, on the other hand, processes data received from the sensory memory (see Fig. 3.1). Since working memory has a limited storage capacity, cognitive (memory) load increases as the new data obtained from the sensory memory accumulates. This results in a loss of information [33] and allows only temporary storage of information. These characteristics are associated with daily tasks such as reasoning, planning, and learning since they require efficient processing and retention of information.

Due to its critical role, working memory needs to be considered separately. In Fig. 3.2, working memory structure we designed for an ego driver is given. The number of environmental vehicles is denoted by N and the number of different driving types is denoted by l. In working memory, we allocated a unit for each vehicle in the environment, resulting in N-many units. In each unit, a sub-unit is dedicated to each driving type, resulting in l-many sub-units. Each sub-unit is represented by M_{ji}, where the observed driver's ID is denoted by $j = 1, 2, \ldots, N$ and the driving types are denoted by $i = 1, 2, \ldots, l$. As pointed out earlier, ego driver's observation of driver j at time t, denoted as r_{jt}, is initially stored in sensory memory before being transferred to working memory for further processing. Then, the value functions $v_i(.)$ that are stored in the long-term memory (see the discussion before Definition 2) are used by the working memory to calculate $v_i(r_{jt})$, which outputs the probability of the driver j to have a driving type-i. Value functions that are used for a specific scenario are detailed in Chapter 4.

Each sub-unit in the working memory has a limited storage capacity, denoted by d. After receiving d-many observation data points and processing them, the content of the sub-unit M_{ji} becomes

$$M_{ji} = \begin{bmatrix} v_i(r_{j_1}) & v_i(r_{j_2}) & \ldots & v_i(r_{j_d}) \end{bmatrix}. \tag{3.1}$$

Since the cognitive load increases due to the limited storage capacity, the entries of M_{ji} are gradually replaced by the new information after d-many time steps. The information obtained at time step $d+1$, $v_i(r_{j_{d+1}})$, replaces the first

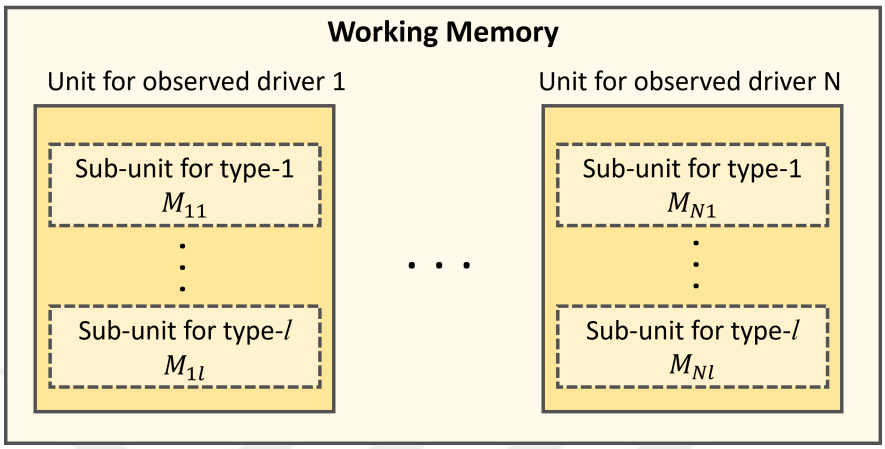

Figure 3.2: Working memory architecture.

entry. Similarly, the information obtained at time step $d+2$, $v_i(r_{j_{d+2}})$, replaces the second entry, and so on. This way, it is ensured that the memory matrix M_{ji} of the working memory always have the information about the last d-many observations.

Consider (3.1). We define a *type score* T_{ji} for each driving type i (see Remark 1) and observed driver with ID j as

$$T_{ji} = ||M_{ji}||_1, \tag{3.2}$$

to determine the driving type of the driver j with the highest probability, where $||\cdot||_1$ is the L_1 norm. If the type score $T_{j\bar{i}}$, $\bar{i} \in \{1, 2, \ldots, l\}$, calculated for type-$\bar{i}$ is the maximum among all T_{ji} values for $i = 1, 2, \ldots, l$, i.e.,

$$\max_i T_{ji} = T_{j\bar{i}}, \tag{3.3}$$

then, the observed type of driver with ID j is determined to be type-$\bar{i}$. This indicates that the ego driver's driving style should be adapted considering an interaction with a type-$\bar{i}$ driver.

3.2 Driver Model with Learning Abilities

Consider the multi-type car following model described in Chapter 2. Defining the position, velocity, and preferred front to back distance ratio of a type-i ego driver (see Remark 1) by $x^{(i)}(t)$, $\dot{x}^{(i)}(t)$, and $\alpha^{(i)}$, denoting the positions and the velocities of the vehicles that are in front of and behind the ego vehicle by $x_f(t)$, $x_b(t)$, $\dot{x}_f(t)$, and $\dot{x}_b(t)$, respectively, and using (2.4) as the basis of the driver model with learning abilities, the dynamics of the type-i driver can be written as

$$\dot{X}^{(i)}(t) = AX^{(i)}(t) + bu_1(t) - \alpha^{(i)}G(X^{(i)}(t) + u_2(t)), \tag{3.4}$$

where $X^{(i)}$ is the state vector defined as

$$X^{(i)}(t) = \begin{bmatrix} x_f(t) - x^{(i)}(t) \\ \dot{x}^{(i)}(t) \end{bmatrix}, \tag{3.5}$$

A, G, and b are defined in (2.5), $u_1(t)$ is given as

$$u_1(t) = \begin{cases} \dot{x}_f(t) & \text{if } v_{min} \leq \dot{x}_f(t) \leq v_{max} \\ v_{min} & \text{if } \dot{x}_f(t) \leq v_{min} \\ v_{max} & \text{if } \dot{x}_f(t) \geq v_{max} \end{cases}, \tag{3.6}$$

and

$$u_2(t) = \begin{bmatrix} u_2^1(t) \\ u_2^2(t) \end{bmatrix}, \tag{3.7}$$

where

$$\begin{aligned} u_2^1(t) &= \begin{cases} \dot{x}_b(t) & \text{if } v_{min} \leq \dot{x}_b(t) \leq v_{max} \\ v_{min} & \text{if } \dot{x}_b(t) \leq v_{min} \\ v_{max} & \text{if } \dot{x}_b(t) \geq v_{max} \end{cases} \\ u_2^2(t) &= \begin{cases} x_f(t) - x_b(t) & \text{if } d_{min} \leq x_f(t) - x_b(t) \leq d_{max} \\ d_{min} & \text{if } x_f(t) - x_b(t) \leq d_{min} \\ d_{max} & \text{if } x_f(t) - x_b(t) \geq d_{max} \end{cases} \end{aligned}, \tag{3.8}$$

and v_{min}, v_{max}, d_{min}, and d_{max} are parameters to be selected based on the conditions of the modeled highway, reflecting the minimum and maximum speeds, and

front vehicle to back vehicle distances considered by the ego driver. The idea behind the modification of the inputs given in (2.6) to the ones given in (3.6)-(3.8) is the following: This modification allows the model to avoid unrealistic and highly improbable scenarios and increases its accuracy and applicability to real-world conditions. By doing so, it ensures that the model operates within the range of realistic observations, such as the natural speed limits of vehicles and the maximum observable distance between the front and back vehicles. Additionally, this way, the model maintains stability, preventing erratic or unpredictable behavior that could arise from unbounded inputs. Consequently, this approach improves both the efficiency and performance of the model, enabling it to better simulate realistic driving conditions.

To implement the learning mechanism, we need to write the dynamics of type-i driver given in (3.4) in a more compact form. To achieve this, we begin by introducing a weight vector $W^{(i)} \in \mathbb{R}^l$, $i = 1, \ldots, l$, defined as

$$W^{(i)} = \begin{bmatrix} \delta_{i,1} & \delta_{i,2} & \ldots & \delta_{i,l-1} & \delta_{i,l} \end{bmatrix}^T, \tag{3.9}$$

where $\delta_{i,k} = 1$ if $i = k$ and $\delta_{i,k} = 0$ otherwise. Then, using (3.9), $X^{(i)}(t)$, defined in (3.4), can be expressed as

$$X^{(i)}(t) = \begin{bmatrix} X^{(1)}(t) & X^{(2)}(t) & \ldots & X^{(l)}(t) \end{bmatrix} W^{(i)}. \tag{3.10}$$

Depending on the driving types of the surrounding vehicle drivers, we assume that there exists an *ideal driving style* for the ego driver that can be expressed as a linear combination of predefined driving types (see Remark 1). Inspired by the expression given in (3.10), an ideal driving style, which we call the *reference model* from now on, can be obtained. To do this, we first define the states of the reference model as

$$X_r(t) = \begin{bmatrix} X^{(1)}(t) & X^{(2)}(t) & \ldots & X^{(l)}(t) \end{bmatrix} W^*, \tag{3.11}$$

where W^* is the weight vector of the ideal driving style, the formation of which is explained in the sequel.

Definition 3: The attention parameters, denoted as θ_f, θ_{ego}, and $\theta_b \in \mathbb{R}^+ \cup \{0\}$, are defined as follows:

1. θ_f: The degree of attention allocated by the ego vehicle towards the front vehicle. It characterizes the extent to which the ego vehicle responds to the actions and movements of the vehicle that is directly ahead of it.

2. θ_{ego}: Defined as the self-attention parameter, this parameter indicates the ego vehicle's focus on its own behavior and driving style. It expresses the tendency of the ego driver to persist in driving with their existing driving type.

3. θ_b: Reflecting the attention towards the vehicle at the back, this parameter signifies the awareness and responsiveness of the ego vehicle to the actions of the vehicle behind it.

Overall, parameters θ_f, θ_{ego}, and θ_b represent the levels of attention that the ego vehicle gives to the front, self, and back vehicles, respectively.

By using the best driving types and the attention parameters defined in Definition 2 and Definition 3, and denoting the front and back vehicles by subscripts f and b, respectively, the ideal weight vector W^* in (3.11) for a car following model having l different driving types can be written as

$$W^* = \begin{bmatrix} \gamma_{1,f} & d_{1,ego} & \gamma_{1,b} \\ \gamma_{2,f} & d_{2,ego} & \gamma_{2,b} \\ \vdots & \vdots & \vdots \\ \gamma_{l,f} & d_{l,ego} & \gamma_{l,b} \end{bmatrix} \begin{bmatrix} \theta_f \\ \theta_{ego} \\ \theta_b \end{bmatrix}, \tag{3.12}$$

where

$$\gamma_{i,j} = \begin{cases} 1 & \text{if type-}i \text{ is the best type against} \\ & \text{the type of the vehicle with ID } j \\ 0 & \text{otherwise} \end{cases}. \tag{3.13}$$

We denote the initial (at the beginning of interactions) driving type of the ego driver by i_{ego} and call it the ego driver's *own* driving type. Then, in (3.12), $d_{i,ego} = 1$ if $i_{ego} = i$ and 0 otherwise. Furthermore, the condition

$$\theta_f + \theta_{ego} + \theta_b = 1 \tag{3.14}$$

should be satisfied to ensure

$$X_r(t) \geq \min(X^{(1)}(t), X^{(2)}(t), \ldots, X^{(l)}(t)) \tag{3.15a}$$

$$X_r(t) \leq \max(X^{(1)}(t), X^{(2)}(t), \ldots, X^{(l)}(t)). \tag{3.15b}$$

The reference model can be obtained by taking the derivative of (3.11) as

$$\dot{X}_r(t) = \begin{bmatrix} \dot{X}^{(1)}(t) & \dot{X}^{(2)}(t) & \ldots & \dot{X}^{(l)}(t) \end{bmatrix} W^*. \tag{3.16}$$

By substituting (3.4), for all types $i = 1, \ldots, l$, into (3.16), and then using (3.11) and $||W^*||_1 = 1$, it can be obtained that (3.16) is equivalent to

$$\dot{X}_r(t) = AX_r(t) + bu_1(t) - u_\alpha(t)W^*, \tag{3.17}$$

where

$$u_\alpha(t) = G \begin{bmatrix} X^{(1)}(t)^T + u_2(t)^T \\ X^{(2)}(t)^T + u_2(t)^T \\ \vdots \\ X^{(l)}(t)^T + u_2(t)^T \end{bmatrix}^T \Lambda, \tag{3.18}$$

A, G and b are given in (2.5), $u_1(t)$ and $u_2(t)$ are defined in (3.6), (3.7) and (3.8), and the constant matrix Λ is given as

$$\Lambda = \begin{bmatrix} \alpha^{(1)} & 0 & \ldots & 0 \\ 0 & \alpha^{(2)} & \ldots & 0 \\ \vdots & & \ddots & \vdots \\ 0 & 0 & \ldots & \alpha^{(l)} \end{bmatrix}. \tag{3.19}$$

At each time instant when the ego driver's inference about the driving type of an observed driver changes, the ideal weight vector W^* is updated (see (3.12)-(3.14)). This update causes an abrupt transition from one state to another, necessitating a strategy to ensure a smooth and realistic transition modeling the learning process. This can be achieved by replacing W^* in (3.17) with the online updated weight vector $W(t)$, which gives us the model for the ego driver as

$$\dot{X}(t) = AX(t) + bu_1(t) - u_\alpha(t)W(t). \tag{3.20}$$

Theorem: The states of the ego driver's model, given in (3.20), converge to those of the reference model, given in (3.17), i.e. $\lim_{t\to\infty} X(t) = X_r(t)$, if the weight vector $W(t)$ is updated using the adaptive law

$$\dot{W}(t) = \gamma u_\alpha(t)^T P e(t), \tag{3.21}$$

where $\gamma \in \mathbb{R}^+$ is the learning rate,

$$e(t) = X(t) - X_r(t) \tag{3.22}$$

is the error between the states of the ego driver and the reference model, and $P \in \mathbb{R}^+_{2\times 2}$ is the unique solution of the Lyapunov equation

$$A^T P + PA = -Q \tag{3.23}$$

for a positive definite symmetric $Q \in \mathbb{R}^+_{2\times 2}$.

Proof: By taking the derivative of the error $e(t)$ defined in (3.22), and using (3.17) and (3.20), we obtain that

$$\begin{aligned} \dot{e}(t) &= \dot{X}(t) - \dot{X}_r(t) \\ &= Ae(t) - u_\alpha(t)(W(t) - W^*) \\ &= Ae(t) - u_\alpha(t)\tilde{W}(t), \end{aligned} \tag{3.24}$$

where $\tilde{W}(t) = W(t) - W^*$. Consider the Lyapunov function candidate

$$V(t) = e(t)^T P e(t) + \gamma^{-1}\tilde{W}(t)^T\tilde{W}(t). \tag{3.25}$$

Taking the derivative of $V(t)$ and using (3.23) and (3.24), it is obtained that

$$\begin{aligned} \dot{V}(t) = &\ \dot{e}(t)^T P e(t) + e(t)^T P \dot{e}(t) \\ &+ \gamma^{-1}\tilde{W}(t)^T\dot{\tilde{W}}(t) + \gamma^{-1}\dot{\tilde{W}}(t)^T\tilde{W}(t) \\ = &\ e(t)^T(A^TP + PA)e(t) + 2\gamma^{-1}\tilde{W}(t)^T\dot{\tilde{W}}(t) \\ &- \tilde{W}(t)^T u_\alpha(t)^T P e(t) - e(t)^T P u_\alpha(t)\tilde{W}(t) \\ = &\ -e(t)^T Q e(t) + 2\gamma^{-1}\tilde{W}(t)^T\dot{\tilde{W}}(t) \\ &- 2\tilde{W}(t)^T u_\alpha(t)^T P e(t). \end{aligned} \tag{3.26}$$

Substituting the adaptive law (3.21) into (3.26), it is obtained that

$$\dot{V}(t) = -e(t)^T Q e(t) \leq 0. \tag{3.27}$$

Therefore, the equilibrium $(e(t) = 0, \tilde{W}(t) = 0)$ is stable in the sense of Lyapunov, and $e(t)$ and $\tilde{W}(t)$ are bounded. From (3.4), $X^{(i)}(t)$'s are bounded for all $i = 1, \ldots, l$ since $A - \alpha^{(i)} G$ is Hurwitz, where A and G are defined in (2.5), and $u_1(t)$ and $u_2(t)$ are bounded inputs. From (3.11), $X_r(t)$ is bounded since $X^{(i)}(t)$'s are bounded for all $i = 1, \ldots, l$ and elements of W^* are in the closed interval $[0, 1]$ (see (3.12)-(3.14)). Since $e(t)$ and $X_r(t)$ are bounded, it follows from (3.22) that $X(t)$ is bounded. Given that $X^{(i)}(t)$'s are bounded for all $i = 1, \ldots, l$, (3.18) implies that $u_\alpha(t)$ is also bounded. Hence, together with the boundedness of $e(t)$ and $\tilde{W}(t)$, it follows from (3.24) that $\dot{e}(t)$ is bounded. Therefore, the second derivative of $V(t)$,

$$\ddot{V}(t) = -2e(t)^T Q \dot{e}(t) \tag{3.28}$$

is bounded, and by Barbalat's Lemma, $\lim_{t\to\infty} e(t) = 0$. Finally, (3.22) indicates that $\lim_{t\to\infty} X(t) = X_r(t)$. ■

Remark 3: The scenario in which the ego driver does not learn, where the driving type remains fixed to the initial type, can be created by setting the learning rate γ in (3.21) to 0. In this case, the model for the ego driver reduces to (3.4), which is stable since $A - \alpha^{(i)} G$ is Hurwitz for all $i = 1, \ldots, l$.

Chapter 4

Simulations

In this Chapter, the methodology followed to determine the model parameters is explained and the performance of the proposed car following model is comparatively analyzed using real human driver behaviors obtained from NGSIM dataset [32].

4.1 Data Processing

We use the vehicle trajectories dataset from the Next Generation Simulation (NGSIM) program [32], which includes position, velocity, ID, and lane information for each vehicle. Since the focus of this paper is car following models, lane-changing events are excluded. At the end, the data of 120 vehicles are extracted from the dataset.

In the NGSIM dataset, the data for all vehicles are not simultaneously available for all time instances. Therefore, we performed interpolation to obtain data for each vehicle at every time step of 0.01 seconds.

4.2 Simulation Setting

In Remark 2, three driving types with related preferred ratio values, $\alpha^{(1)} = 0.5$, $\alpha^{(2)} = 1$, and $\alpha^{(3)} = 2$, are explained. In this chapter, the same driving types are utilized, with the corresponding best types, as elaborated in Definition 2. Therefore, type-1 and type-3 are the best types against each other, and type-2 is the best type against itself. The driving types are visualized in Fig. 4.1.

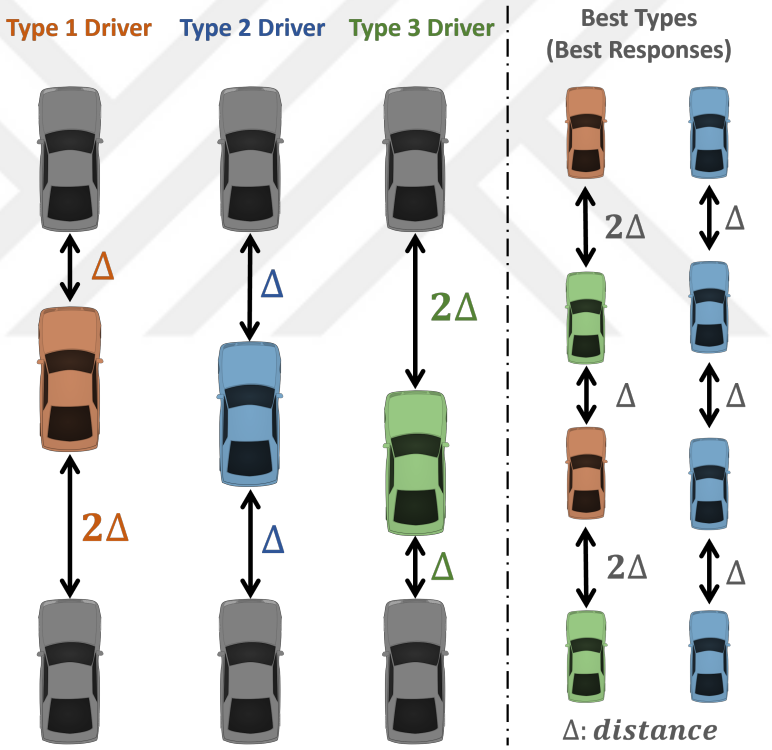

Figure 4.1: Types and the best type (best response) definitions are visualized. Type 1, 2, and 3 drivers are represented by orange, blue, and green, respectively.

The bounds v_{max}, v_{min}, d_{max} and d_{min} in (3.6) and (3.8) are selected as 33m/s ($\sim$ 120km/h), 0m/s, 200m and 3m, respectively. The maximum velocity of 33m/s represents typical highway speed limits, reflecting the maximum speed that the ego driver is likely to observe. The minimum velocity of 0m/s accounts for stationary vehicles in traffic jams and stop-and-go scenarios. A maximum distance of 200m reflects a typical visibility region and ensures the ego driver is influenced only by the vehicles that are close enough. The minimum distance of 3m handles

close proximity situations, reflecting safe following distances at low speeds.

The value functions in (3.1) are constructed by using the intervals explained in Remark 2. Therefore, type-1, type-2 and type-3 are matched with ratio intervals $I_1 = (0.3, 0.7)$, $I_2 = (0.7, 1.4)$ and $I_3 = (1.4, 2.6)$, respectively. To determine the intervals, the symmetry around the $\alpha^{(1)} = 0.5$ and $\alpha^{(3)} = 2$ values is considered. Front to back distance ratios of the vehicles in the front r_{f_t} and at the back r_{b_t} at time instant t are the inputs to the value functions. Using these, the value functions in (3.1) are constructed as

$$v_i(r_{j_t}) = \begin{cases} h_i(r_{j_t}) & \text{if } r_{j_t} \in I_i \\ 0 & \text{otherwise} \end{cases} \tag{4.1}$$

where

$$h_1(r_{j_t}) = 1 - e^{-\beta_1(r_{j_t}-0.3)^2} - e^{-\beta_1(r_{j_t}-0.7)^2} \tag{4.2a}$$

$$h_2(r_{j_t}) = 1 - e^{-\beta_2(r_{j_t}-0.7)^2} - e^{-\beta_2(r_{j_t}-1.4)^2} \tag{4.2b}$$

$$h_3(r_{j_t}) = 1 - e^{-\beta_3(r_{j_t}-1.4)^2} - e^{-\beta_3(r_{j_t}-2.6)^2} \tag{4.2c}$$

with the parameters $\beta_1 = 500$, $\beta_2 = 200$, and $\beta_3 = 100$. These parameters ensure that the output of the value function $v_i(\cdot)$ associated with type-i takes its maximum value in the region around the preferred ratio $\alpha^{(i)}$ and decreases to 0 when the observed ratio exits the ratio interval I_i. Value functions are visualized in Fig. 4.2.

The idea behind selecting this value function structure is the following. The importance of a data point for a driver decreases as the data approaches the boundaries of the intervals it is matched with. This is because the driver cannot be certain and assigns a smaller probability to the estimated type.

As described in Section 3.1, the assigned values are stored in separate memory sub-units for each type, resulting in three memory sub-units for each observed driver (see Fig. 3.2). The capacity of working memory is a debated topic. While some studies, such as [34], suggest that it can hold seven data points, others, like [35], argue that this number ranges between 3 and 5. In this work, the memory structure is designed to have five data slots in each sub-unit. It is noted that

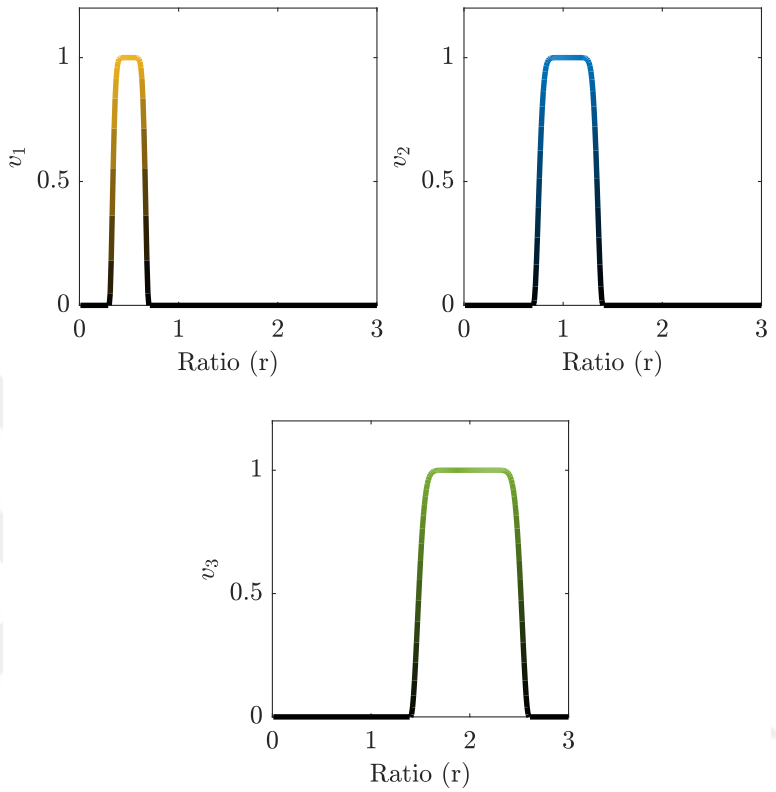

Figure 4.2: Value functions: Type-1 (left), Type-2 (middle), Type-3 (right) for $r = r_{j_t}$.

unlike car-following models, for models that incorporate lane interactions, the vehicles on the adjacent lanes must also be observed. Data from these vehicles should be stored in dedicated memory units to accurately model traffic dynamics.

4.3 Identification of Driver Parameters

In the attention based learning mechanism described in Chapter 3, there are 4 parameters, consisting of attention parameters θ_f, θ_{ego}, θ_b, and the learning rate γ, for each driver (see Definition 3 and (3.21)). To identify these parameters for individual drivers, a 60-second data from the NGIM dataset is used. The initial driving types are obtained by checking the average front to back distance ratios for the first 2 seconds of the 60-second simulation period. For the rest of the

simulation, the front to back distance ratios of the vehicles in front and at the back of each modeled vehicle, extracted from the NGSIM data, are used as the input r_{j_t} for the value function described in (4.1) and (4.2).

Four parameters, θ_f, θ_{ego}, θ_b, and γ, which minimize the position error between the model and the data, are identified for each 120 driver in the dataset by using simulated annealing. The output of the simulated annealing algorithm are the unnormalized attention values $\bar{\theta}_f$, $\bar{\theta}_{ego}$, $\bar{\theta}_b$, and the learning rate γ, where $\bar{\theta}_j \in [0, 1]$ for all $j \in \{f, ego, b\}$ and $\gamma \in [0, 10]$. The attention parameters are then obtained as $\theta_j = \bar{\theta}_j / (\Sigma_j \bar{\theta}_j)$ to satisfy (3.14).

4.4 Analysis of Driver Parameter Distributions: Kolmogorov-Smirnov Goodness of Fit Test

We want to show that the driver models produced by the proposed approach are general enough to represent different sets of traffic data. To achieve this, we randomly divided the driver data into two, each of which contains 60 drivers. Then, we made a goodness-of-fit analysis to demonstrate that the parameter distributions in these two sets of data are statistically similar.

Kolmogorov-Smirnov (K-S) Test is a nonparametric hypothesis testing method used to determine whether a set of samples is coming from a hypothesized distribution (one-sample K-S Test) or two sets of samples are coming from the same distribution (two-sample K-S Test). In this section, we use the two-sample K-S Test to evaluate whether the distributions of the learning rates and the attention parameters (see Section 4.3) are consistent between the two datasets. To do this, we set our null hypothesis as follows:

H_0: The parameters obtained for both datasets are sampled from the same probability distribution.

It is noted that the result of the K-S Test does not conclude that the null hypothesis is correct. Instead, it provides a decision to either *reject* or *not reject* the null hypothesis. Therefore, if the decision is to *not reject* the null hypothesis, then there is not enough evidence to conclude that the two datasets are sampled from different distributions, and we retain the hypothesis. . This decision is made by comparing the p-value obtained by the test with a predetermined *significance level* α_{ks} which is selected as $\alpha_{ks} = 0.05$ in this study. A p-value less than α_{ks} indicates that the null hypothesis is rejected.

To test the hypothesis, first, the learning rate (see (3.21)) distributions are compared using the one-dimensional K-S Test [36] resulting in a p-value of 0.24 and retaining the null hypothesis. Second, the distribution of the attention parameters (see Definition 3) is compared using the multidimensional version of the K-S Test by Fasano and Franceschini [37]. Since the attention parameters satisfy (3.14), θ_b can be written in terms of θ_f and θ_{ego}, indicating that using the two-dimensional distribution of θ_f and θ_{ego} is enough. The two-sample, two-dimensional K-S Test is implemented using [38], which resulted in a p-value of 0.39, leading to retaining the null hypothesis. This result suggests that the distributions of model parameters in different datasets have similar characteristics.

4.5 Comparing Learning and Fixed Models

The purpose of this section is to exemplify the advantage of incorporating learning in the proposed model. To achieve this, we use one of the driver's data randomly selected from the NGSIM dataset [32], and compare the predictive capabilities of the fixed model developed in Chapter 2 with the learning model given in Chapter 3. The attention parameters in (3.12) and the learning rate in (3.21) are obtained using the method described in Section 4.3. The results of the 60-seconds simulations are given in Fig. 4.3, where the predicted and real "front-to-back distance ratio" and "distance to the front vehicle" are depicted. Each time instant that the reference model for the learning model, given in (3.17), is updated is marked in the figure. These updates occur due to the changes in

the estimated type of observed drivers. As shown in the figure, the model with learning has dramatically better prediction performance, compared to the fixed model. Furthermore, the figure demonstrates the importance of the transient learning dynamics, by showing the discrepancy between the "ideal model" (reference model) and the real data, and how this gap is closed by introducing learning dynamics.

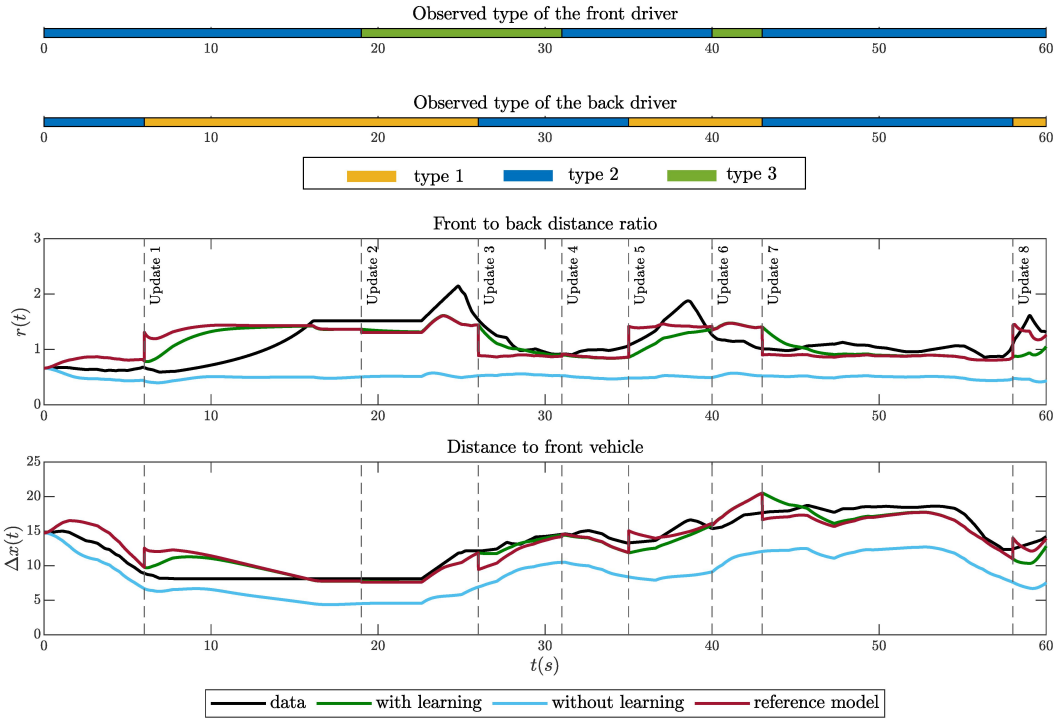

Figure 4.3: 60 seconds simulation result for a driver in the dataset comparing the trajectories of the models without learning and with learning. Two color bars at the top show the types of front and back drivers observed by the ego driver. Black vertical dashed lines represent the moments that a type change in one of the front or back vehicles is observed. This change causes the ideal weight vector to be updated (see (3.12) and (3.13)). Therefore, the reference model (shown by the red line in the following plots) is updated at that time instants by using the information of new observed types. Front to back distance ratio $r(t) = \frac{x_f(t)-x(t)}{x(t)-x_b(t)}$ plot shows that, unlike the learning model, a fixed (non-learning) model cannot achieve the desired distance ratio by the driver extracted from the data. Distance to front vehicle $\Delta x(t) = x_f(t) - x(t)$ plot shows that the model with learning abilities represents the data observed from a driver's trajectory better than the model without learning.

4.6 Comparison with Intelligent Driver Model (IDM)

In this section, real human driver behaviors obtained from NGSIM dataset [32] are compared with the multi-type car following model without learning (Chapter 2), with attention-based learning mechanism (Chapter 3), and *Intelligent Driver Model (IDM)* [6], which is a commonly used car following model, such as in [8, 9, 20, 25]. In IDM, the acceleration of a vehicle is expresses as

$$a(t) = a_{max}\left[1 - \left(\frac{v(t)}{v_{max}}\right)^4 - \left(\frac{s^*(t)}{s(t)}\right)^2\right] \tag{4.3}$$

where

$$s^*(t) = s_0 + Tv(t) - \frac{v(t)\Delta v(t)}{2\sqrt{a_{max}b_{des}}} \tag{4.4}$$

is the desired distance to the front vehicle, a_{max} is the maximum acceleration, b_{des} is the desired (comfortable) deceleration, T is the desired time headway, s_0 is the minimum distance to front vehicle, v_{max} is the maximum velocity which is taken as $120km/h$ ($\sim 33m/s$) since it is slightly above the speed limit on the highway that the data is collected, and $a(t)$, $v(t)$, $\Delta v(t) = v_f(t) - v(t)$ and $s(t)$ are the ego vehicle's current acceleration, velocity, velocity difference with the front vehicle and distance to front vehicle.

The analysis is conducted separately on two different datasets, each comprising 60 drivers. Since the model parameters of the car-following model with learning are determined using simulated annealing (see Section 4.3), the same approach is applied to identify IDM parameters to ensure a fair comparison. The free parameters of the IDM are a_{max}, b_{des}, T, and s_0, which are given in Table 4.1 together with the bounds used in optimization. These bounds are chosen in accordance with the ones used in [39]. Then, the trajectories of the vehicles are obtained using the optimized parameters.

To compare the models, the average *Root Mean Square Error (RMSE)* between the actual position data of the vehicles and the positions predicted by the driver models are calculated. The results obtained for the first dataset are shown in

Parameter		Bounds
a_{max}	Maximum acceleration	[0.1,4]
b_{des}	Desired deceleration	[0.1,4]
T	Desired time headway	[0.1,3]
s_0	Minimum distance to front vehicle	[0.1,3]

Table 4.1: Table of IDM parameters and bounds.

Table 4.2. In the table, the model without learning is taken as baseline and the RMSE error improvements obtained using IDM and the model with learning are given.

Model	Average RMSE	Improvement
without learning	3.56 m	-
IDM	2.98 m	16.3%
with learning	2.61 m	26.6%

Table 4.2: RMSE errors between real position data (dataset 1), and model outputs.

The findings presented in Table 4.2 can be interpreted from two perspectives. Firstly, in trajectory prediction, the model with attention-based learning mechanism outperforms IDM. While both the IDM and the proposed model with learning has 4 adjustable parameters, due to the relationship described in (3.14), one of the attention parameters can be expressed in terms of the other two. This effectively reduces the number of independent parameters in the learning mechanism to 3. Thus, the proposed model utilizes fewer independent parameters, while providing a better representation of driver behavior. Secondly, integrating the attention-based learning mechanism into the multi-type car-following model led to a significant 26.7% reduction in trajectory error, compared to the case without learning. This demonstrates the potential of incorporating a human-like learning mechanism in driver models to enhance their performance.

To ensure consistency and verify that comparable results are achieved across

different datasets, the identical procedure is applied to the second dataset. The results are given in Table 4.3, where similar conclusions can be drawn.

Model	Average RMSE	Improvement
without learning	3.63 m	-
IDM	3.19 m	12.1%
with learning	2.77 m	23.7%

Table 4.3: RMSE errors between real position data (dataset 2), and model outputs.

Chapter 5

Parameter Classification & Simulator Design

5.1 Classification of Model Parameters

To create a high-fidelity simulation, a model that fits a given dataset is not enough. This may lead to over-fitting and lack generalization. Instead, we need a model that can generate a diverse set of driver behaviors that are general enough to capture the diversity in real driving behavior. In Section 4.4, we showed that parameter distributions of the proposed model across two different datasets are statistically similar. This reveals that the model can capture the general structure of real life driving behavior. In this section, we go one step further and show how the model parameters can be classified in such a way that these classifications can be used later in creating a reliable simulation environment, which is detailed in the following section. The following subsections will detail the classification methods employed, including k-means clustering and the Gaussian mixture model.

5.1.1 K-means Clustering of the Parameters

The k-means clustering method is a widely used statistical analysis technique that groups data into different classes, called clusters, based on their distances to the center points of the groups, called centroids [40]. To implement this method, first, we reorganize the data in three dimensions, which are the front and self attention parameters θ_f and θ_{ego}, and the normalized learning rate $\gamma/10$. The normalization of the learning rates is needed to have the range $[0, 1]$ in all dimensions. It is noted that the attention parameter θ_b is not included in the analysis since it can be derived from (3.14) using θ_f and θ_{ego}. Each data point is denoted by an index $s = 1, \ldots, 120$ as $d_s = (\theta_f, \theta_{ego}, \gamma/10)_s$. The second step is determining the number of clusters. For this, the elbow method is used [41]. To employ this method, the sums of squared distances of all the data points to the centroids of the cluster they are in, called inertia and denoted by I, are calculated by using the formula

$$I(K) = \sum_{k=1}^{K} \sum_{d_s \in S_k} d(d_s, c_k)^2, \tag{5.1}$$

for $K = 1, \ldots, 10$. K is the number of clusters, the optimum value of which is to be found. Furthermore, S_k is the set of data points in cluster k, and $d(d_s, c_k)$ is the Euclidean distance between the data point d_s and the centroid c_k. The inertia values calculated in (5.1) for different values of K are shown in Fig. 5.1, on the left. The values of the cost function

$$C(K) = w_1 K + w_2 I(K), \tag{5.2}$$

where $w_1 = 0.6$ and $w_2 = 0.4$ are given in Fig. 5.1, on the right. The weights can be selected depending on the specific application. In our case, we decided to weigh having fewer clusters slightly more heavily than the inertia, to eliminate unnecessary amount of clusters. (See [41] and [42] for the details of implementing k-means clustering and weighted sum scalarization.)

As seen from Fig. 5.1, on the right, the number of clusters that minimize the cost curve is $K = 5$. Fig. 5.2 shows the data points, five clusters, and their centroids.

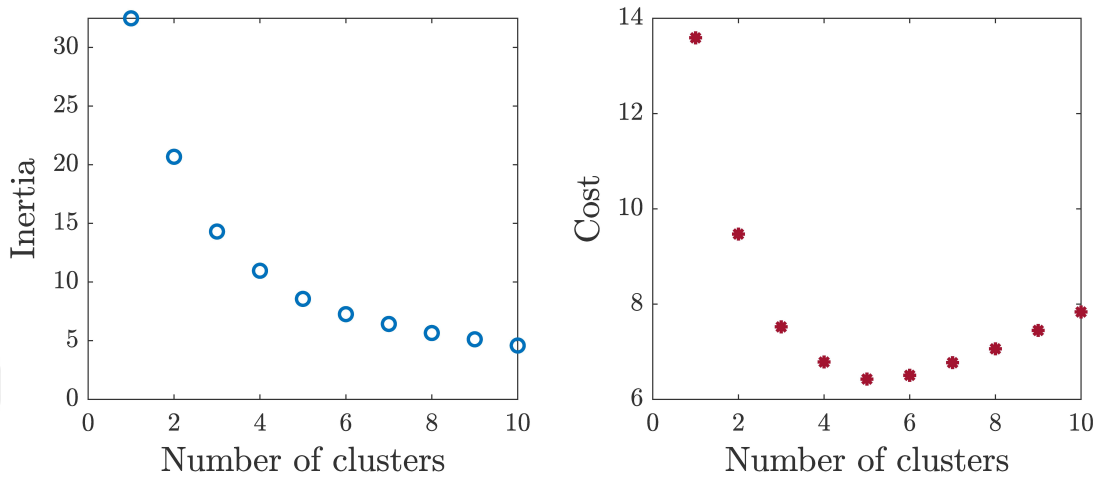

Figure 5.1: Elbow technique and weighted sum scalarization.

The results of the k-means clustering method are also provided in Table 5.1. In this table, "Ratio" refers to the percentage of data points that belong to a specific cluster. For example, the table shows that 15% of the drivers fall into the cluster with centroid $(0.57, 0.16, 0.09)$. In the table, we also provide the percentages of "initial types" of the drivers in a given cluster (for driving types, see Remark 1). These types are calculated using the first 2 seconds of the traffic data (Initial type information is used when developing a simulator, which is explained in the next section.). It is indicated in the table that among the drivers that belong to the cluster with a centroid $(0.57, 0.16, 0.09)$, 22% have an initial driving type of Type-1, while the percentages for Type-2 and Type-3 are 61% and 17%, respectively.

Ratio	Centroid	Type-1	Type-2	Type-3
15%	$(0.57, 0.16, 0.09)$	22%	61%	17%
20.8%	$(0.10, 0.32, 0.31)$	32%	60%	8%
17.5%	$(0.06, 0.76, 0.81)$	10%	66%	24%
22.5%	$(0.06, 0.85, 0.26)$	11%	67%	22%
24.2%	$(0.36, 0.22, 0.77)$	31%	52%	17%

Table 5.1: Table of k-means clustering results and the initial driving type analysis.

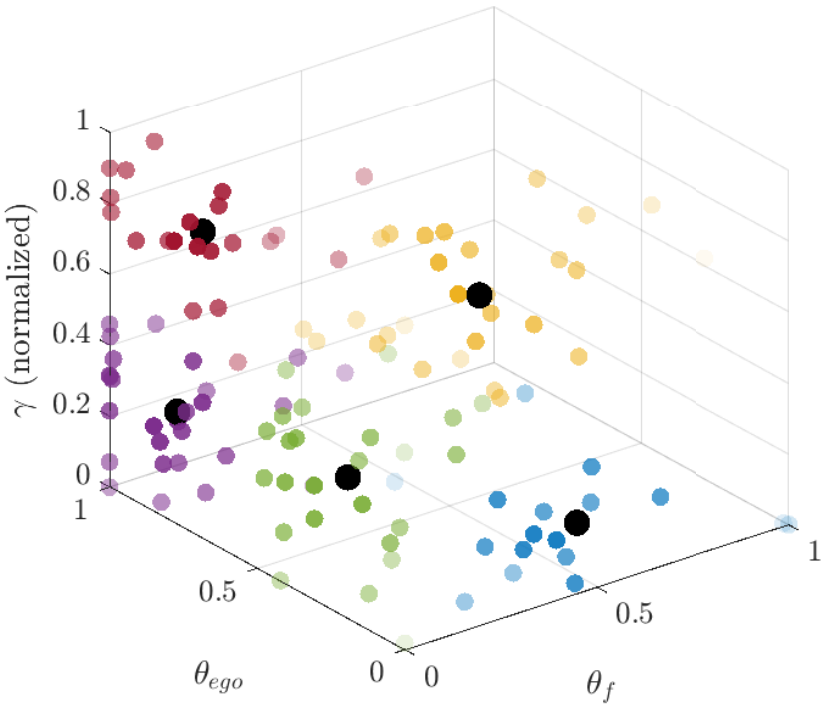

Figure 5.2: k-means clustering results for five clusters. Each color indicates a different cluster. Centroids are shown with black points.

5.1.2 Gaussian Mixture Model of the Parameters

Gaussian Mixture Model (GMM) is a clustering method that is commonly used in statistical analysis [43]. Unlike the k-means clustering method, GMM considers the data points as drawn from a mixture of different Gaussian distributions, each of which constitutes a separate cluster. Therefore, in GMM, the clusters does not have strict boundaries, allowing the representation of more complex data patterns.

Just as with the k-means clustering method, determining the number of clusters, which are also called "components", is crucial for a GMM to ensure that it is neither overly complex nor inadequate in representing the data. Akaike Information Criterion (AIC) is used to determine the number of components [44].

The AIC value is defined as

$$AIC = 2k - 2\log(\hat{L}), \tag{5.3}$$

where k is the number of model parameters and $\hat{L}$ is the maximum value of the likelihood function showing how well the model parameters represent given data. According to this criterion, the number of components that minimize the AIC value, which are shown in Fig. 5.3, should be selected.

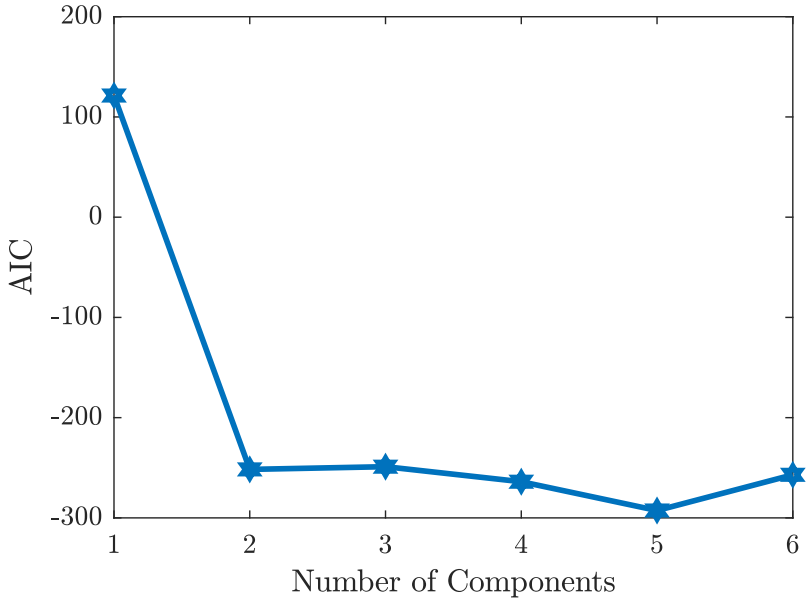

Figure 5.3: AIC values for different number of components.

Based on AIC results, the data is divided into five components using GMM algorithm. The information of each component is given in Table 5.2. In the table, "Mixing coefficient" refers to the percentage of data points that belong to a specific component, and type-i, $i = 1, 2, 3$, are the initial driving types of the drivers (see Remark 1) identified using the first 2 seconds of the traffic data. The features provided for each component can be used in creating a simulator, which is explained in the following section.

	Component 1	Component 2	Component 3
Mixing Coefficients	40%	23%	15%
Mean Point	$(0, 0.62, 4.70)$	$(0.41, 0.24, 6.78)$	$(0.54, 0.15, 0.64)$
Covariance Matrix	$\begin{bmatrix} 0 & 0 & 0.0003 \\ 0 & 0.0976 & -0.0603 \\ 0.0003 & -0.0603 & 8.0032 \end{bmatrix}$	$\begin{bmatrix} 0.0353 & -0.0087 & 0.1334 \\ -0.0087 & 0.0289 & 0.1334 \\ 0.1334 & 0.1334 & 4.3217 \end{bmatrix}$	$\begin{bmatrix} 0.0595 & -0.0138 & -0.0343 \\ -0.0138 & 0.0212 & -0.0231 \\ -0.0343 & -0.0231 & 0.5646 \end{bmatrix}$
Type-1 Ratio	17%	32%	22%
Type-2 Ratio	69%	47%	72%
Type-3 Ratio	14%	21%	6%

	Component 4	Component 5
Mixing Coefficients	18%	4%
Mean Point	$(0.19, 0.75, 4.89)$	$(0.08, 0.19, 5.02)$
Covariance Matrix	$\begin{bmatrix} 0.0182 & -0.0162 & -0.0400 \\ -0.0162 & 0.0207 & -0.0137 \\ -0.0400 & -0.0137 & 10.7235 \end{bmatrix}$	$\begin{bmatrix} 0.0016 & 0.0033 & -0.0664 \\ 0.0033 & 0.0071 & -0.1193 \\ -0.0664 & -0.1193 & 6.8645 \end{bmatrix}$
Type-1 Ratio	0	100%
Type-2 Ratio	67%	0%
Type-3 Ratio	33%	0%

Table 5.2: Table of Gaussian mixture model parameters and the distribution of initial driving types of drivers in each component.

To visualize the data generation capabilities of GMM, 2500 data points are generated using the information given in Table 5.2. The generated data points are shown in Fig. 5.4, together with real data points used to obtain the GMM. It is noted that, unlike the k-means clustering method, normalization of the learning rate γ is not necessary for GMM since the covariance matrices are naturally adjusted to scale the spread of data across dimensions.

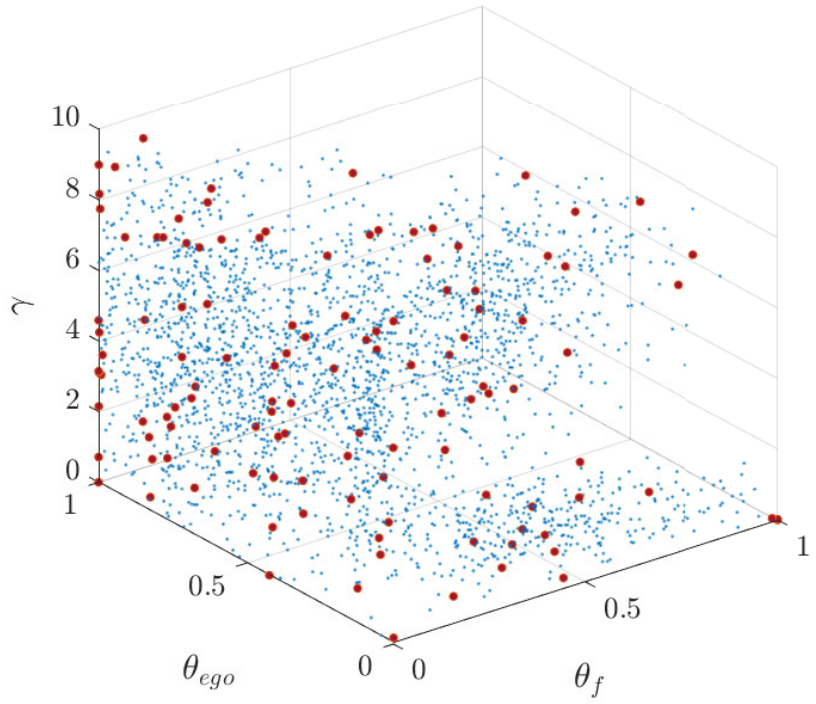

Figure 5.4: Gaussian mixture model. Red points represent the existing data points (experimental data). Blue points are generated by using the Gaussian mixture model.

5.2 Roadmap for Designing a Traffic Simulator

In this section, we provide insights into how to design a traffic simulator using the described attention-based learning mechanism. An overview of the steps and their contents are given in Fig. 5.5, and the details are explained below.

Determining the External Inputs

In this thesis, the attention-based learning mechanism is combined with a car-following model which directed the discussion to considering the vehicles on a single lane. However, the model can be used to model a highway, considering all the lanes separately. The first step of designing a simulator using the proposed

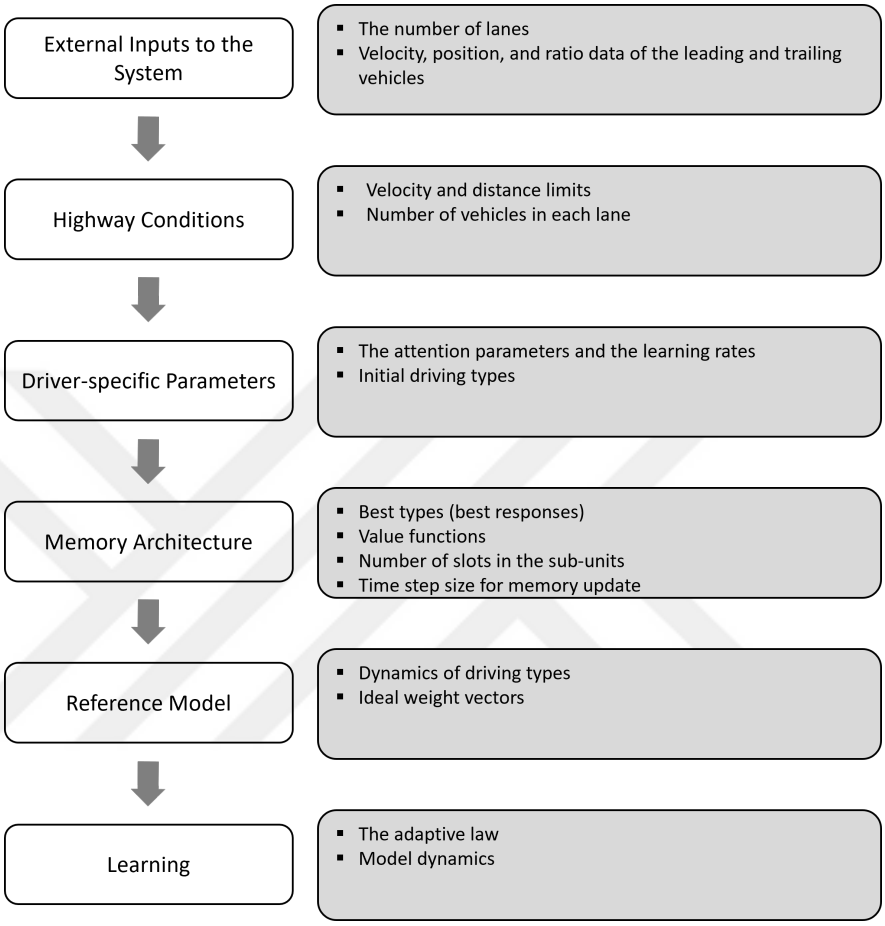

Figure 5.5: Steps of the simulator design process using the attention-based learning mechanism.

model is to determine the number of lanes to be modeled. For each lane, the velocities, positions, and front distance to back distance ratios of the vehicles at the very front and back of the lane are needed. These can be obtained from traffic data using an inference framework. It is noted that we model the vehicles in between these leading and trailing vehicles, which we call *vehicles of interest* (see Chapter 2).

Determining the Highway Conditions

The limits of the considered velocities and distance between the vehicle in front and at the back should be determined. These parameters are denoted by v_{min},

v_{max}, d_{min}, and d_{max} in (3.6) and (3.8). Additionally, the number of drivers to be modeled and the drivers' initial positions and velocities should be determined.

Determining the Driver-specific Parameters

The driver-specific parameters are the attention parameters θ_f, θ_{ego} and θ_b defined in Definition 3, the learning rate γ used in (3.21), and the initial driving types of the drivers, which is required to construct the ideal weight vector given in (3.12). To determine these parameters, the following two methods can be used:

K-means clustering, discussed in Section 5.1.1

This method is suitable when the application does not require a large variety in driver behavior. In other words, if only a few different driving styles are enough, then this method is ideal.

To use this method, the attention parameters and the learning rates should be selected for each driver by using Table 5.1. In this table, the information related to five different clusters is given. The drivers in the specific clusters should have the parameters described by the centroids. The first and the second elements of the centroids express the θ_f and θ_{ego} values, and the third element is the learning rate γ. The third attention parameter θ_b should satisfy (3.14). Drivers can be assigned to these clusters using the ratios given in Table 5.1. Within each cluster, the initial types can be determined using the values in the same table.

Gaussian mixture model, given in Section 5.1.2

This model is ideal for scenarios where a large range of diverse driver behavior is desired. In this method, the attention parameters in (3.12) and the learning rates in (3.21) should be sampled using Table 5.2. By using the mixing coefficients, mean points and covariance matrices, data points can be generated as shown in

Fig. 5.4. To satisfy the model requirements, the following constraints must be applied to the generated data points.

$$0 \leq \theta_f \leq 1 \tag{5.4a}$$

$$0 \leq \theta_{ego} \leq 1 \tag{5.4b}$$

$$\theta_f + \theta_{ego} \leq 1 \tag{5.4c}$$

$$0 \leq \gamma \leq 10. \tag{5.4d}$$

Similar to k-means clustering method, (3.14) needs to be used to find θ_b. The initial driving types can be distributed using the ratios given in Table 5.2.

Remark 4: Depending on the purpose of the simulation, one can select the model parameters independent of the statistical distribution of model parameters based on real traffic data. This maybe, for example, to test certain edge cases. For example, one can create an environment consisting of aggressive drivers who always try to keep a very small following distance, with large learning rates. Or, one may want to model novice drivers who show inconsistent learning rates with varying following distances. This can be achieved by, for example, randomly selecting attention parameters and learning rates. These variations can be helpful in creating a comprehensive test environment for autonomous driving algorithms. It is noted that in any case, the attention parameters should satisfy (3.14) and the learning rate γ should be positive or 0.

Building the Memory Architecture

The preferred ratio values and the best responses given in Definition 1 and Definition 2 should be used to define the driving types (see Remark 1) and the best types (see Remark 2). The intervals given in Remark 2 can be used to construct the value functions, which are required for (3.1), if custom value functions are desired. Otherwise, the value functions given in (4.1) and (4.2) can be used. This completes the formation of the long-term memory unit, explained in Section 3.1.

The number of slots in each sub-unit of the working memory and the time step size that new information will be processed and added to the memory matrix (3.1)

related to each sub-unit should be selected. We suggest using five slots and a one-second step time in accordance with [34] and [35]. Then, the type score should be calculated using (3.2), and the observed types of the drivers should be identified using (3.3). This completes the formation of the working memory unit.

Constructing the Reference Model

The reference model states given in (3.11) require two types of information to be known: 1) The dynamics of each driving type that is created using (3.10), and 2) the ideal weight vector given in (3.12).

First, the inputs given in (3.6), (3.7) and (3.8) should be determined. Then, by using preferred ratio values for different types (see Remark 2), and A, G, and b defined in (2.5), the dynamics of each type can be obtained using (3.10).

Obtaining the ideal weight vector (3.12) requires the information of observed driving types of other drivers, which is obtained from the memory architecture explained in the sub-section above, and the parameters determined in Section 5.2. Then, by using (3.13) and the explanation below it, (3.12) can be calculated.

Incorporating Learning

Driver dynamics can be obtained by using (3.20), which requires the dynamics of driving types, model inputs, A, G, and b, and the weight vector $W(t)$ to be known. Except for $W(t)$, the creation of all the other components is explained in the previous sub-section.

To obtain the weight vector $W(t)$ using (3.21), first, its initial value must be known, which can be found using the initial types of the drivers and (3.9). Then, the error given in (3.22), and u_α given in (3.18) should be calculated. Finally, the P matrix can be found using (3.23). Then, we can calculate $W(t)$ and use it in (3.20) to model the learning period.

Chapter 6

Conclusion and Future Works

In this thesis, an attention-based learning mechanism is introduced, and integrated into a multi-type car-following model we developed. The comparison between models with and without this learning mechanism revealed a significant improvement in predicting real human driving trajectories, highlighting the importance of accounting for human learning. An in-depth analysis of the model parameters is conducted using goodness-of-fit statistical tests, providing valuable insights into the model's capability of capturing general driver behavior characteristics. Additionally, a step by step explanation on how to implement the proposed model is provided.

6.1 Summary of the Contributions

In the context of car following and driver modeling, significant research has been dedicated to representing human driver behaviors with increasing accuracy. Despite these advances, a notable gap persists: the integration of human-like learning mechanisms into driver models. Existing models often capture driver behavior under specific conditions but fail to account for the dynamic nature of driving style changes. Human drivers continuously observe, understand, and adapt based

on their experiences, a feature that is crucial for realistic modeling.

This thesis addresses this gap by incorporating a human-inspired memory architecture into driver models, demonstrating that emulating the human learning process enhances model accuracy. The integration of this mechanism allows for dynamic adaptation of driving styles and better reflects the complexity of human behavior. Our model, which updates itself online and represents diverse driving styles, is both simple to implement and computationally efficient. This is a significant improvement over existing models that typically use the same parameters for all drivers, thereby limiting the diversity of driving behaviors.

Additionally, our work includes the impact of the vehicle behind the ego vehicle, an aspect often neglected in the literature. By considering this influence, our model offers a more comprehensive view of how surrounding vehicles affect driving behavior.

In conclusion, this research provides valuable tools for creating traffic simulators, and also encourages further exploration of human learning in other applications. We believe that our work will inspire researchers to continue working on models that better mimic human learning and adaptation.

6.2 Future Works

The attention-based learning mechanism developed in this thesis has been successfully integrated into a multi-type car following model. Extending this integration to other multi-type driver models could lead to substantial performance enhancements. Notably, this learning mechanism is not confined to car-following models alone; its application can be explored in multi-type driver models that exhibit lane-changing behaviors, offering a promising direction for future research.

To enhance the realism and accuracy of the proposed mechanism, future research could integrate additional cognitive processes, such as handling uncertainty

and emotional responses. This would involve modeling how drivers react to various types of distractions, which could arise from observing unexpected behaviors of other drivers, encountering challenging road conditions, or dealing with adverse weather. By incorporating these elements, researchers could gain a deeper understanding of the cognitive processes involved in driving, allowing for a more comprehensive simulation of human driving behaviors.

Bibliography

[1] N. Kalra and S. M. Paddock, "Driving to safety: How many miles of driving would it take to demonstrate autonomous vehicle reliability?," *Transportation Research Part A: Policy and Practice*, vol. 94, pp. 182–193, 2016.

[2] K. Zhang, C. Chang, W. Zhong, S. Li, Z. Li, and L. Li, "A systematic solution of human driving behavior modeling and simulation for automated vehicle studies," *IEEE Transactions on Intelligent Transportation Systems*, 2022.

[3] R. C. Atkinson and R. M. Shiffrin, "Human memory: A proposed system and its control processes," in *Psychology of learning and motivation*, vol. 2, pp. 89–195, Elsevier, 1968.

[4] A. D. Baddeley, G. J. Hitch, and R. J. Allen, "From short-term store to multicomponent working memory: The role of the modal model," *Memory & cognition*, vol. 47, pp. 575–588, 2019.

[5] P. G. Gipps, "A behavioural car-following model for computer simulation," *Transportation research part B: methodological*, vol. 15, no. 2, pp. 105–111, 1981.

[6] M. Treiber, A. Hennecke, and D. Helbing, "Congested traffic states in empirical observations and microscopic simulations," *Physical review E*, vol. 62, no. 2, p. 1805, 2000.

[7] H. Yeo and A. Skabardonis, "Understanding stop-and-go traffic in view of asymmetric traffic theory," in *Transportation and Traffic Theory 2009:*

Golden Jubilee: Papers selected for presentation at ISTTT18, a peer reviewed series since 1959, pp. 99–115, Springer, 2009.

[8] M. Park, Y. Kim, and H. Yeo, "Development of an asymmetric car-following model and simulation validation," *IEEE Transactions on Intelligent Transportation Systems*, vol. 21, no. 8, pp. 3513–3524, 2019.

[9] M. Shang, B. Rosenblad, and R. Stern, "A novel asymmetric car following model for driver-assist enabled vehicle dynamics," *IEEE Transactions on Intelligent Transportation Systems*, vol. 23, no. 9, pp. 15696–15706, 2022.

[10] C. Wei, E. Paschalidis, N. Merat, A. Solernou, F. Hajiseyedjavadi, and R. Romano, "Human-like decision making and motion control for smooth and natural car following," *IEEE Transactions on Intelligent Vehicles*, 2021.

[11] R. Wiedemann, "Simulation des strassenverkehrsflusses.," 1974.

[12] D.-A. Nguyen, J. Nwadiuto, H. Okuda, and T. Suzuki, "Modeling car-following behavior in downtown area based on unsupervised clustering and variable selection method," in *2020 IEEE International Conference on Systems, Man, and Cybernetics (SMC)*, pp. 3714–3720, IEEE, 2020.

[13] Z. Xing, X. Liu, D. Cui, J. Zhou, and H. Fu, "Parameters identification research of stylized car-following models based on behavior clustering," in *2022 IEEE 2nd International Conference on Data Science and Computer Application (ICDSCA)*, pp. 566–572, IEEE, 2022.

[14] Y. Li, B. Chen, H. Zhao, S. Peeta, S. Hu, Y. Wang, and Z. Zheng, "A car-following model for connected and automated vehicles with heterogeneous time delays under fixed and switching communication topologies," *IEEE Transactions on Intelligent Transportation Systems*, vol. 23, no. 9, pp. 14846–14858, 2021.

[15] S. Wang, B. Yu, and M. Wu, "Mvcm car-following model for connected vehicles and simulation-based traffic analysis in mixed traffic flow," *IEEE Transactions on Intelligent Transportation Systems*, vol. 23, no. 6, pp. 5267–5274, 2021.

[16] D. Lin and L. Li, "An efficient safety-oriented car-following model for connected automated vehicles considering discrete signals," *IEEE Transactions on Vehicular Technology*, 2023.

[17] W. Lu, Z. Yi, B. Liang, Y. Rui, and B. Ran, "Learning car-following behaviors for a connected automated vehicle system: An improved sequence-to-sequence deep learning model," *IEEE Access*, vol. 11, pp. 28076–28089, 2023.

[18] M. F. Ozkan and Y. Ma, "Modeling driver behavior in car-following interactions with automated and human-driven vehicles and energy efficiency evaluation," *IEEE Access*, vol. 9, pp. 64696–64707, 2021.

[19] M. F. Ozkan and Y. Ma, "Trust-aware control of automated vehicles in car-following interactions with human drivers," in *2022 IEEE 61st Conference on Decision and Control (CDC)*, pp. 5279–5284, IEEE, 2022.

[20] X. Wen, S. Jian, and D. He, "Modeling the effects of autonomous vehicles on human driver car-following behaviors using inverse reinforcement learning," *IEEE Transactions on Intelligent Transportation Systems*, 2023.

[21] A. Zhou, Y. Liu, E. Tenenboim, S. Agrawal, and S. Peeta, "Car-following behavior of human-driven vehicles in mixed-flow traffic: A driving simulator study," *IEEE Transactions on Intelligent Vehicles*, 2023.

[22] A. Adewale and C. Lee, "Prediction of car-following behavior of autonomous vehicle and human-driven vehicle based on drivers' memory and cooperation with lead vehicle," *Transportation research record*, vol. 2678, no. 6, pp. 248–266, 2024.

[23] W. Schwarting, A. Pierson, J. Alonso-Mora, S. Karaman, and D. Rus, "Social behavior for autonomous vehicles," *Proceedings of the National Academy of Sciences*, vol. 116, no. 50, pp. 24972–24978, 2019.

[24] W. Si, T. Wei, and C. Liu, "Agen: Adaptable generative prediction networks for autonomous driving," in *2019 IEEE Intelligent Vehicles Symposium (IV)*, pp. 281–286, IEEE, 2019.

[25] Y. Yu, Z. He, and X. Qu, "On the impact of prior experiences in car-following models: model development, computational efficiency, comparative analyses, and extensive applications," *IEEE transactions on cybernetics*, 2021.

[26] K. Shaheen, M. A. Hanif, O. Hasan, and M. Shafique, "Continual learning for real-world autonomous systems: Algorithms, challenges and frameworks," *Journal of Intelligent & Robotic Systems*, vol. 105, no. 1, pp. 1–32, 2022.

[27] B. Wickramasinghe, G. Saha, and K. Roy, "Continual learning: A review of techniques, challenges and future directions," *IEEE Transactions on Artificial Intelligence*, 2023.

[28] Y. Wu, H. Tan, X. Chen, and B. Ran, "Memory, attention and prediction: a deep learning architecture for car-following," *Transportmetrica B: Transport Dynamics*, vol. 7, no. 1, pp. 1553–1571, 2019.

[29] Y. Liao, G. Yu, P. Chen, B. Zhou, and H. Li, "Modelling personalised car-following behaviour: a memory-based deep reinforcement learning approach," *Transportmetrica A: transport science*, vol. 20, no. 1, p. 2035846, 2024.

[30] M. R. Hajidavalloo, Z. Li, D. Chen, A. Louati, S. Feng, and W. B. Qin, "Mechanical system inspired microscopic traffic model: Modeling, analysis, and validation," *IEEE Transactions on Intelligent Vehicles*, vol. 8, no. 1, pp. 301–312, 2022.

[31] L. Xu, J. Ma, and Y. Wang, "A car-following model considering the effect of following vehicles under the framework of physics-informed deep learning," *Journal of Advanced Transportation*, vol. 2022, no. 1, p. 3398862, 2022.

[32] U. D. of Transportation Federal Highway Administration, "Next generation simulation (ngsim) vehicle trajectories and supporting data," tech. rep., Provided by ITS DataHub through Data.transportation.gov, 2016. `http://doi.org/10.21949/1504477`.

[33] A. D. Baddeley, "Working memory," *Philosophical Transactions of the Royal Society of London. B, Biological Sciences*, vol. 302, no. 1110, pp. 311–324, 1983.

[34] G. A. Miller, "The magical number seven, plus or minuars two: Some limits on our capacity for processing information.," *Psychological review*, vol. 63, no. 2, p. 81, 1956.

[35] N. Cowan, "The magical number 4 in short-term memory: A reconsideration of mental storage capacity," *Behavioral and brain sciences*, vol. 24, no. 1, pp. 87–114, 2001.

[36] F. J. Massey Jr, "The kolmogorov-smirnov test for goodness of fit," *Journal of the American statistical Association*, vol. 46, no. 253, pp. 68–78, 1951.

[37] G. Fasano and A. Franceschini, "A multidimensional version of the kolmogorov–smirnov test," *Monthly Notices of the Royal Astronomical Society*, vol. 225, no. 1, pp. 155–170, 1987.

[38] B. Lau, "2-d kolmorogov-smirnov test, n-d energy test, hotelling t2 test," *GitHub, Retrieved July 6, 2024*, 2024. `https://github.com/brian-lau/multdist`.

[39] A. Alhariqi, Z. Gu, and M. Saberi, "Calibration of the intelligent driver model (idm) with adaptive parameters for mixed autonomy traffic using experimental trajectory data," *Transportmetrica B: transport dynamics*, vol. 10, no. 1, pp. 421–440, 2022.

[40] D. Arthur and S. Vassilvitskii, "k-means++: The advantages of careful seeding," tech. rep., Stanford, 2006.

[41] T. M. Kodinariya, P. R. Makwana, *et al.*, "Review on determining number of cluster in k-means clustering," *International Journal*, vol. 1, no. 6, pp. 90–95, 2013.

[42] R. T. Marler and J. S. Arora, "The weighted sum method for multi-objective optimization: new insights," *Structural and multidisciplinary optimization*, vol. 41, pp. 853–862, 2010.

[43] G. J. McLachlan and D. Peel, *Finite mixture models*, vol. 299. John Wiley & Sons, 2000.

[44] J. E. Cavanaugh and A. A. Neath, "The akaike information criterion: Background, derivation, properties, application, interpretation, and refinements," *Wiley Interdisciplinary Reviews: Computational Statistics*, vol. 11, no. 3, p. e1460, 2019.